ELSEVIER

Biochimica et Biophysica Acta 1509 (2000) 440–450

BIOCHIMICA ET BIOPHYSICA ACTA
BBA

www.elsevier.com/locate/bba

The effect of dimethyl sulphoxide on the structure and phase behaviour of palmitoleoylphosphatidylethanolamine

Zhi-Wu Yu [a,b], Peter J. Quinn [a,*]

[a] *Division of Life Sciences, King's College London, 150 Stamford Street, London SE1 8WA, UK*
[b] *Department of Chemistry, Tsinghua University, Beijing 100084, PR China*

Received 18 May 2000; received in revised form 25 August 2000; accepted 5 September 2000

Abstract

The thermotropic phase behaviour and structure of a nonbilayer-forming lipid, 1-palmitoyl-2-oleoyl-phosphatidylethanolamine, dispersed in water and in aqueous solutions of up to 50 wt% dimethyl sulphoxide (DMSO) have been characterised using synchrotron X-ray diffraction methods. It was found that the presence of DMSO in the solvent induced an increase in the temperature of lamellar-gel to lamellar-liquid-crystal phase transition and a decrease in the temperature of the lamellar-liquid-crystal to inverted-hexagonal phase transition of the phospholipid. The presence of DMSO also caused a decrease in the X-ray repeat spacings of all the phases studied. Electron density profiles of the phospholipid dispersed in water and 50 wt% DMSO in the bilayer gel state were calculated. The presence of 50 wt% DMSO caused the apparent disappearance of the solvent layer separating phospholipid bilayers in the gel state. The results suggest that DMSO contributes to the bilayer electron density profile and that the amphiphilic solvent molecules partition into the interfacial region.

Keywords: Phase behaviour; Biomembrane thickness; Phospholipid; Electron density profile; X-ray diffraction

1. Introduction

The ability of many cosolutes, such as trehalose, glycerol, and dimethyl sulphoxide (DMSO), to modulate the properties of biomembranes is believed to be the principal mechanism that underlies many of their biological functions. Phospholipids dispersed in aqueous media have been widely employed to model the effects of cosolutes on cell membranes [1–5]. Such studies have included detailed investigations of the interactions between DMSO and phospholipid bilayers [6–10]. Particular interest in DMSO can be attributed to its wide applications in cell biology as a cryoprotectant, membrane permeability enhancer, and a cell fusogen (for reviews see [11–13]).

The molecular mechanisms responsible for the various effects of DMSO on membranes have yet to be precisely defined. Previous studies in our laboratory have shown that DMSO can induce significant shrinkage of repeat spacing of phospholipid liposomes [14]. Calculation of electron density profiles of dipalmitoylphosphatidylcholine (DPPC) showed an apparent increase in the bilayer thickness [15]. Since there were no significant differences between wide-angle X-ray scattering (WAXS) profiles recorded for gel phase of phospholipid dispersed in water or 35 wt% DMSO, it was argued that any contribution to the effect of DMSO on bilayer thick-

* Corresponding author. Fax: +44-207-848-4500; E-mail: p.quinn@kcl.ac.uk

0005-2736/00/$ – see front matter
PII: S0005-2736(00)00326-6

ness due to a change in the angle of tilt of the acyl chains would be small. The data were interpreted as an orientation of DMSO about the phospholipid head groups located in the interfacial region such that the sulphur and phosphorus atoms both contribute to the regions of high X-ray scattering in the repeat structure. Subsequent calculations of electron density distributions across the bilayer repeat of DPPC multilayer dispersions [7,9] have confirmed that the thickness of the solvent layer separating the bilayers is drastically reduced in the presence of DMSO but neither study found any significant changes in bilayer thickness of DPPC in the gel state. Tristram-Nagle and coworkers [7], however, showed that at temperatures less than 20°C a stable subgel phase was induced by the presence of DMSO which was characterised by a greater bilayer thickness than the usual subgel phase formed by DPPC. They attributed this to a different head group ordering and smaller chain tilt. Shrinkage of the solvent layer interposed between phospholipid bilayers was said to be due to dehydration of the lipid beyond that resulting from replacement of water by DMSO, i.e. an increase in DMSO:H_2O in the interlamellar space. The changes in calculated relative electron density of the solvent layer versus the phosphate group region in the presence of DMSO were unexplained. Another study using molecular simulation methods also concluded that there were no significant changes of the lipid bilayer thickness when DMSO replaced water as solvent [10]. It is noteworthy, however, that the simulation time was only 2 ns and this may be too short to observe penetration of DMSO in between the lipid head groups as this would be expected to be a relatively slow process [16].

Most of the studies of DMSO on model membranes to date have been undertaken with phosphatidylcholines which have different solvation properties compared to nonbilayer-forming lipids such as phosphatidylethanolamines. The present work aimed to characterise the structure and thermotropic phase behaviour of phosphatidylethanolamine dispersed in excess aqueous DMSO solutions. Particular emphasis was devoted to assess the contribution of chain tilt to bilayer thickness. Synchrotron X-ray diffraction methods were used in the study so that both static and dynamic parameters could be derived. We were able to assess the effect of DMSO on the repeat spacing of the multilamellar phases formed by the phospholipid and from this we performed electron density calculations across the bilayer repeat. The contribution of sulphur atoms of DMSO to the total electron density profiles of the bilayer structure could be identified by this method. By subjecting the dispersions to temperature scans we were able to characterise the structural changes that take place during transitions between phases as well as determine transition temperatures. The results indicate that DMSO has a marked effect on the structure and phase behaviour of phosphatidylethanolamine and this is likely to influence the amphipathic balance within the lipid bilayer matrix of biological membranes in which nonbilayer-forming lipids are a significant component.

2. Materials and methods

Synthetic 1-palmitoyl-2-oleoyl-*sn*-phosphatidylethanolamine (POPE) was purchased from Avanti Polar Lipids Inc. (Birmingham, AL, USA) and was used without further purification. Anhydrous DMSO was purchased from Sigma Chemical Co. (St. Louis, MO, USA). Lipid dispersions with a lipid/solvent ratio of 1:3 (w/w) were employed to ensure solvent excess. Homogeneous dispersions were obtained by subjecting the samples to several freeze-thaw cycles between about −20°C and 70°C, interspersed with extensive vortex mixing.

Measurements of synchrotron X-ray diffraction were carried out at Station 8.2 of the Synchrotron Radiation Source at the Daresbury Laboratory, UK, with procedures described previously [17]. Two camera configurations were used to collect the small-angle X-ray diffraction data, namely a short camera (0.1 m) and a long camera (1 m). X-ray scattering intensity was recorded using a multiwire quadrant delay line detector. Data were acquired in 512 consecutive time frames of 3 or 3.5 s separated by a dead time between frames of 50 ms. Experimental data were processed using the OTOKO software (EMBL, Hamburg, Germany) program. Scattering intensities were corrected for fluctuations in beam intensity and detector response recorded from an ^{55}Fe radioactive source. Spatial calibrations were obtained using wet rat-tail collagen (repeat distance

$d = 67$ nm) and fully hydrated DPPC interspersed with Teflon. In calculating the electron density profiles, small-angle scattering intensities were normalised by multiplying a Lorentz factor of $\sin(\theta)$, where θ is the half diffraction angle. Reciprocal spacing $S = 1/d = 2\sin(\theta)/\lambda$ was used for scattering data presentation throughout, where $\lambda = 0.154$ nm is the wavelength of the synchrotron radiation beam at Station 8.2 of Daresbury Laboratory, UK.

Exposure of samples to the X-ray bean was kept to a minimum to avoid possible radiation damage. Visual examination of the samples after measurements showed no change in appearance and measurements performed during successive thermal scans showed no change in thermotropic phase behaviour of the lipid to indicate any sample deterioration.

With a Fourier transform of the diffraction data, electron density distributions across the unit cell of the lamellar repeat of POPE dispersed in both water and aqueous DMSO solution (50 wt%) in the gel state at 10°C can be obtained by the method described previously [15]. Briefly, the electron density function in one-dimensional space x, in arbitrary units, assuming a centre-symmetric structure of the multilayer liposomes, is expressed as follows:

$$\rho(x) = \sum g(h)|F(h)| \cos(2\pi hx/d) \quad (1)$$

where $F(h)$ is the structure factor and equates to the root of the integrated diffraction intensity $I(h)$. For a range of diffraction orders (h), $g(h)$ is the phase of $F(h)$ of the hth order diffraction, and d is the repeat spacing of the multibilayers. The phase problem was addressed by analysing the $F(h)$ function of a swelling series in reciprocal space, based on the Shannon sampling theorem [18,19]. Two experimental approaches were used to assign phase angles to each reflection of the lamellar structures. Measurements were made of a series of samples prepared with limiting solvent. Care was required to ensure that the data were obtained from the reflections from gel phase of the lipid as there was a marked tendency of the lipid to transform into a crystal phase of a type previously reported in phosphatidylcholine [7] in the presence of low amounts of solvent. A second method used data from samples subjected to freeze-induced dehydration which undergo swelling when heated above 0°C. Data obtained from aqueous dispersions and dispersions of the lipid in 50 wt% DMSO using both methods gave consistent results and when incorporated into calculations of electron density distribution produced profiles expected of multibilayer structures.

3. Results

3.1. POPE in excess water

Real-time X-ray diffraction patterns of a dispersion of POPE in pure water recorded during a heat-

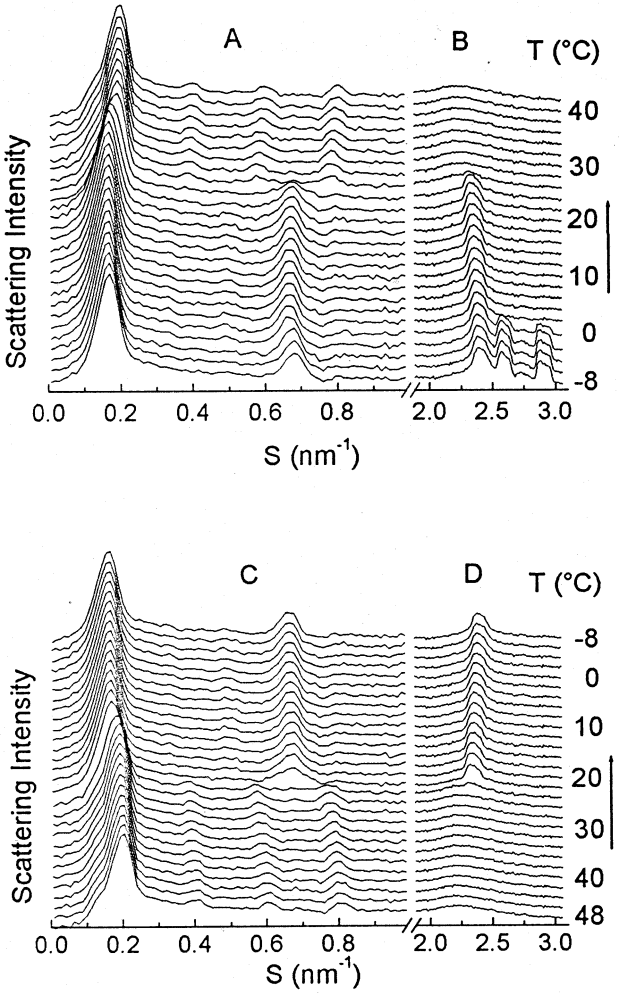

Fig. 1. Plots of successive SAXS (A, C) and WAXS (B, D) intensity profiles versus reciprocal spacing recorded from a dispersion of POPE in excess water during a heating scan (A, B) and the immediate cooling scan (C, D) at 5°/min. Each profile represents a temperature interval of 2°C.

ing scan from −8°C to 40°C are shown in Fig. 1. At low temperatures, two scattering maxima can be observed in the small-angle region of the scattering profile (Fig. 1A). The reciprocal spacing S values of these Bragg reflections are in a ratio of 1:4. The small-angle X-ray scattering (SAXS) patterns are seen to undergo a change at approximately 25°C, in which the two scattering peaks are replaced by four distinct scattering bands. Analysis of their S values showed a ratio of 1:2:3:4. These results suggested that the lipid was arranged in a lamellar structure before and after the phase transition.

WAXS patterns (Fig. 1B) show at least three scattering maxima at −8°C, all but one of which disappeared upon heating above 0°C. The remaining peak persists up to a temperature of 26°C, whereupon it is replaced by a broad scattering band. The multiple peaks below 0°C correspond with those from hexagonal ice. The spacing of 0.42–0.43 nm ($S \approx 2.4$–2.3 nm^{-1}) indicated that the lamellar phase at low temperatures is a gel phase, in which the hydrocarbon chains are packed in a regular hexagonal lattice, while the high-temperature phase, typified by the broad maximum around 0.46 nm ($S \approx 2.2$ nm^{-1}) characteristic of disordered hydrocarbons, is a lamellar liquid-crystal phase.

Subsequent cooling of the dispersion results in a reversal of the phase transition sequence as shown in Fig. 1C,D. The absence of multiple scattering bands at temperatures below 0°C can be attributed to a supercooling effect. The phase transition temperature recorded during heating was 26°C, which is in good agreement with calorimetric data of 25°C [20] and 25.3°C [21], and ^{2}H-NMR studies of 26°C [22]. There is a small temperature hysteresis on cooling, as the liquid-crystal to gel phase transition temperature is 24°C, some 2° lower than recorded during heating. This could be due to the relatively fast scanning rates (5°/min) used in these experiments which were designed to minimise exposure of the sample to the incident X-ray beam.

Heating the dispersion to temperatures above about 65°C induces another phase characterised by reciprocal spacing in a ratio of $1:\sqrt{3}:2$. This is illustrated in Fig. 2, which shows X-ray scattering intensity profiles at temperatures about the phase transition region. This transition is interpreted to be a lamellar liquid-crystal to inverted-hexagonal (H_{II}) phase transition.

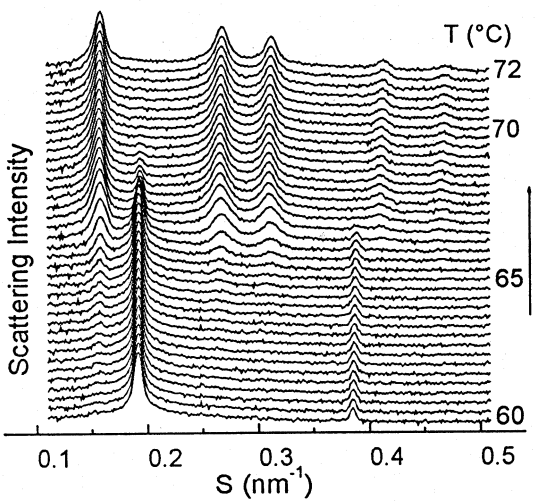

Fig. 2. Plots of successive SAXS intensity profiles versus reciprocal spacing of POPE dispersed in water recorded during a heating scan at a rate of 5°/min, showing a phase transition from lamellar liquid-crystal phase (L_α) to an inverted hexagonal phase (H_{II}).

The dynamics of the lamellar to H_{II} phase transition are shown in more detail in Fig. 3. Changes in intensity of the first-order Bragg scattering peaks during heating are presented in Fig. 3A and a plot of normalised X-ray scattering intensity as a function of temperature is shown in Fig. 3B. The phase transition temperature can be determined by a method widely used in thermal analysis, namely, the determination of the onset temperature. This is the intercept between the baseline represented by the scattering intensities before the phase transition and a line drawn along the progressive change in the scattering intensities during phase transition (Fig. 3B). A phase transition temperature of 65.5°C is obtained by this method. This compares with a value of 71°C obtained by calorimetry [20] but consistent with ^{2}H-NMR data, which gave a midpoint of the phase transition of 65°C [22]. An analogous method can be used to determine the end-point of the phase transition, and this was found to be 66.8°C. Thus the transition region where coexistence of the lamellar and H_{II} phases is observed is 1.3° at a heating rate of 5°/min.

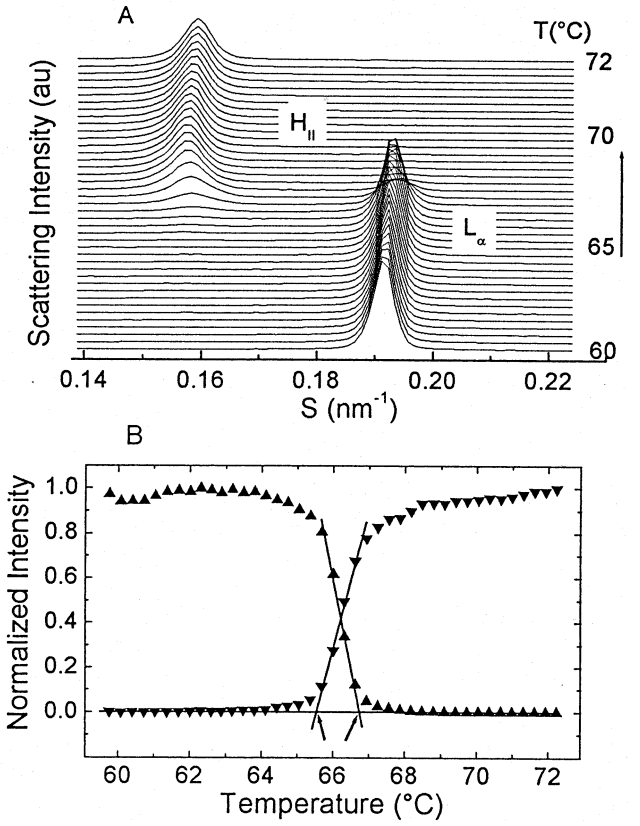

Fig. 3. (A) Plots of successive SAXS intensity profiles versus reciprocal spacing in the region of first-order reflections from a dispersion of POPE in water, showing lamellar to nonlamellar phase transitions. Each diffraction intensity profile represents scattering accumulated in 3.5 s during a heating scan of 5°/min. (B) Normalised X-ray scattering intensities of the lamellar (▲) and nonlamellar (▼) peaks plotted as a function of temperature to show progress of the phase transition. Arrows indicate the positions of onset and completion temperatures, respectively, of the phase transition.

3.2. POPE in DMSO solutions

The effect of DMSO on the phase behaviour of POPE has been examined with regard to three parameters: the phase transition temperature, temperature span of the transition, and the repeat spacing of the bilayer structures. First, replacing pure water with aqueous DMSO solutions caused an increase in the temperature of the L_β to L_α phase transition dependent on the proportion of DMSO in water. Data on phase transition temperatures of POPE dispersed in DMSO solutions, as onset temperatures, are presented in Table 1. The dynamic feature of the phase transition is also illustrated in Figs. 3–5, which shows that the temperature range of coexistence of the lamellar and H_{II} phases increases from 1.3° to 2.6° in the presence of 5 wt% DMSO. When the concentration of DMSO is increased to 40 wt%, the initial L_β phase coexists with the H_{II} phase at temperatures at

Table 1
Phase transition temperatures (°C) of POPE dispersed in excess DMSO aqueous solutions

wt% DMSO	0	5	10	40
L_β to L_α	26	27	29	30
L_α to H_{II}	65.5	63.4		L_β to H_{II}

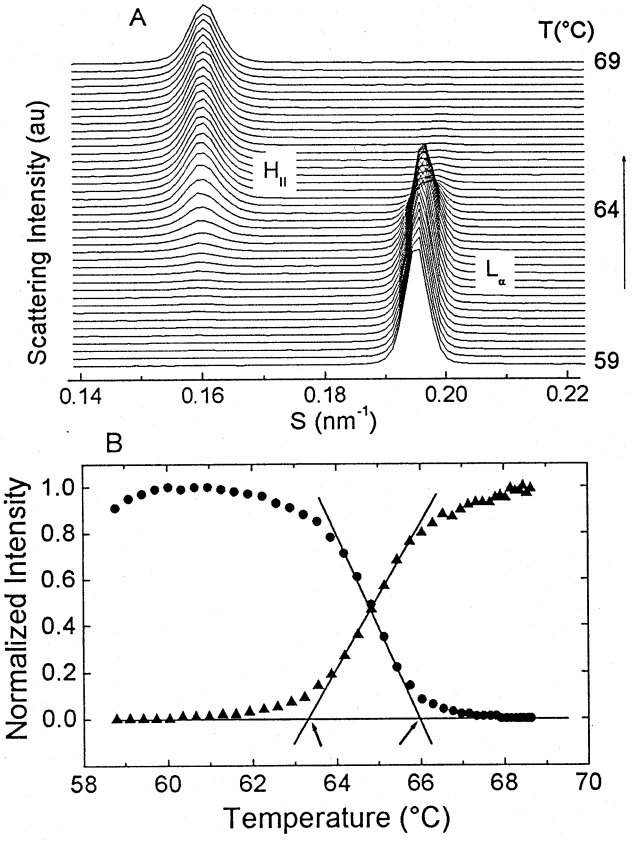

Fig. 4. (A) Plots of successive SAXS intensity profiles versus reciprocal spacing in the region of first-order reflections from a dispersion of POPE in 5 wt% DMSO aqueous solution, showing lamellar to nonlamellar phase transitions. Each diffraction intensity profile represents scattering accumulated in 3.5 s during a heating scan of 5°/min. (B) Normalised X-ray scattering intensities of the lamellar (●) and nonlamellar (▲) peaks are plotted as a function of temperature to show progress of the phase transition. Arrows indicate the positions of onset and completion temperatures, respectively, of the phase transition.

least up to 83°C which was the upper limit of temperature recorded in the experiment shown in Fig. 5.

Once the different phases had been characterised from an index of the higher-order scattering bands, SAXS experiments were performed using a long camera configuration giving a resolution of reciprocal spacing of 0.0011 nm^{-1}. This corresponds to a spacing resolution better than 0.047 nm in this study. The repeat spacing of the multilayer structures of POPE recorded during heating scans at 5°/min in the absence and presence of DMSO are shown in Fig. 6. The repeat spacing of all phases decreases with increasing temperature. For POPE dispersed in water, the repeat spacing of the lamellar-gel L_β phase is 6.31 ± 0.04 nm at 15°C and 6.24 ± 0.04 nm at 23°C, and that of the L_α phase is 5.56 ± 0.04 nm at 26°C and 5.16 ± 0.03 nm at 68°C. The repeat spacing of the H_{II} phase is greater than the lamellar phases and is 6.43 ± 0.04 nm at 64°C and 6.14 ± 0.04 nm at 80°C.

Increasing concentrations of DMSO in the solvent mixture result in a progressive decrease in the repeat spacing of all the phases. At 23°C, L_β phase spacings of 6.24, 6.16 and 5.83 nm of POPE dispersed in 0, 5 and 40 wt% DMSO were recorded, respectively. The effect of DMSO on the spacings of liquid-crystal phases is more significant. The lamellar spacing of 5.16 nm of the dispersion in water at 68°C was reduced to 4.68 nm when water was replaced by 40 wt% DMSO. Similar reductions in repeat spacings due to the presence of DMSO can also be seen in the nonlamellar phase.

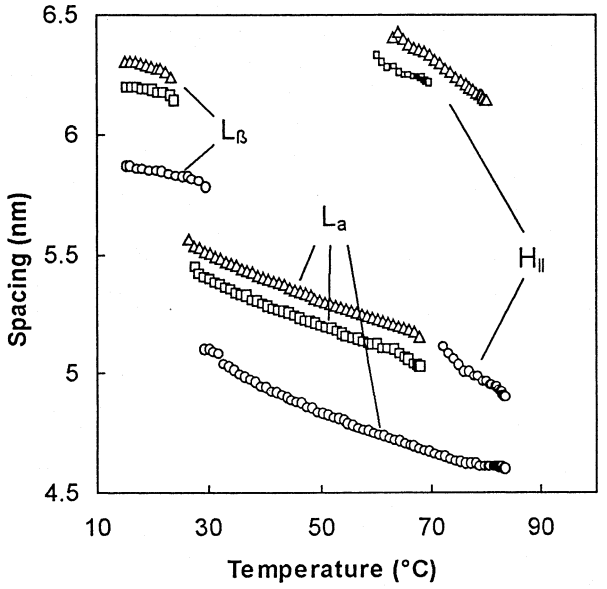

Fig. 6. Repeat spacings of different phase structures (L_α, L_β, and H_{II}) of POPE dispersed in excess aqueous DMSO solutions, with concentrations of 0 wt% (△), 5 wt% (□), and 40 wt% (○). First-order diffraction peaks identified from the long-camera configuration were used to determine the respective spacings.

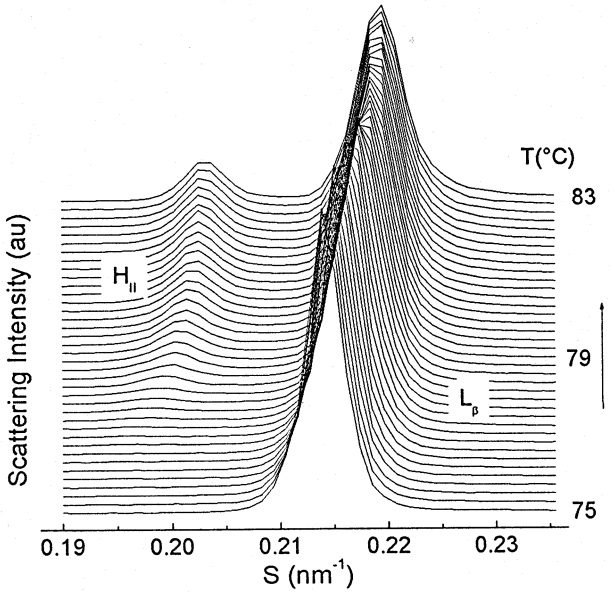

Fig. 5. Plots of successive SAXS intensity profiles versus reciprocal spacing in the region of first-order reflections from a dispersion of POPE in 40 wt% DMSO aqueous solution. Data represent scattering accumulated in 3.5 s during a heating scan of 5°/min, showing the coexistence of the lamellar-gel phase with the newly formed hexagonal phase.

The effect of DMSO on the structure of bilayers of POPE has been examined by calculating electron density profiles across the bilayer repeat of L_β phase of the phospholipid dispersed in both water and aqueous DMSO solutions. Two experimental methods were used to obtain a swelling series to solve the phase problem as described in Section 2. It can be seen from the data in Fig. 7A,B that all the structure factors obtained from dispersions in both water and DMSO solutions fall on a smooth curve. The similarity of these curves implies that the lipid bilayers in the presence and absence of DMSO share similar centrosymmetric structures. The fact that the structure in water and aqueous DMSO is similar suggests that DMSO is able to replace water normally hydrating of the polar head group of phospholipid

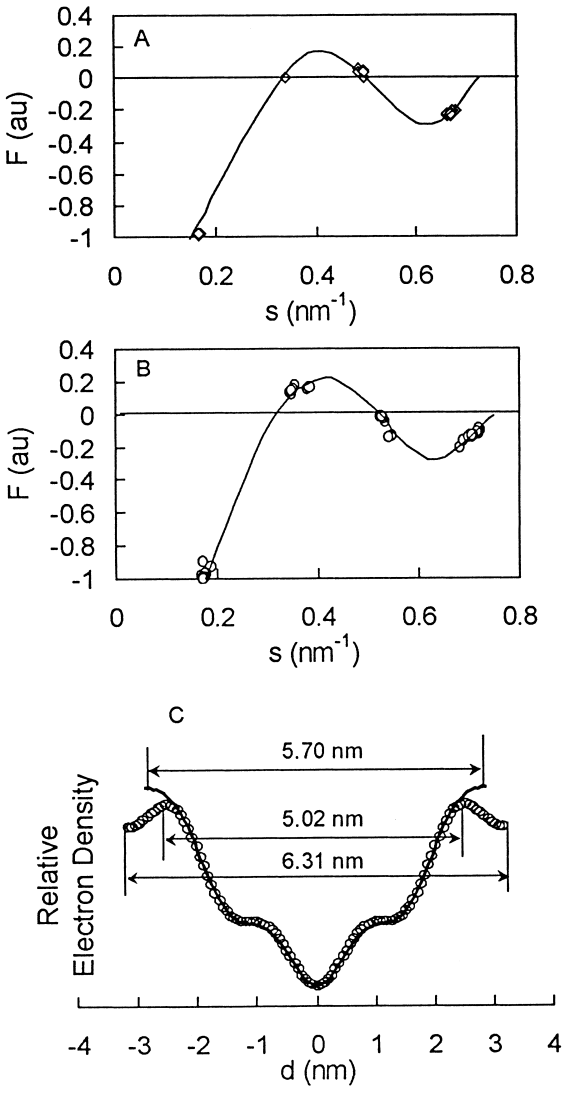

Fig. 7. Structure factors of L_β phase of a dispersion of POPE in H_2O (A) and POPE dispersed in 50 wt% aqueous DMSO (B) obtained from a swelling series (see text for details). (C) Electron density profiles of cross-bilayer structures of L_β phase of POPE dispersed in excess water (○) and 50 wt% DMSO solution (solid line).

[5]. The resulting phase angles used to perform the Fourier synthesis for lipid in water were −++− and for lipid in 50 wt% DMSO were −+−−. One further assumption has been made in the calculations, namely that the electron density in the centre of the bilayer where the lipid tails meet is less than that of water.

An electron density profile of POPE in water was then constructed from Eq. 1 using the phase signs derived from the first four orders of reflection of the swelling series. The low-resolution profile resulting from this calculation is shown in Fig. 7C. Using these data, a peak-to-peak distance of 5.02 nm is obtained, representing the phosphorus–phosphorus distance. This gives an apparent water layer thickness of 1.29 nm in space separating consecutive bilayers. This is close to the value of 1.33 nm obtained in a study of the lamellar-gel phase of dilauroylphosphatidylethanolamine dispersed in water reported by McIntosh and Simon [23].

The electron density profiles across the bilayer structure of POPE dispersed in 50 wt% DMSO solution are also shown in Fig. 7C. This shows that, in addition to the shorter lamellar repeat spacing, the peak-to-peak distance is increased by more than 0.5 nm due to the presence of DMSO and the solvent layer has apparently disappeared. To determine whether the increase in the apparent bilayer thickness is due to any change of the angle of tilt of the acyl chains, wide-angle X-ray diffraction intensities of the dispersions were examined and the data are presented in Fig. 8. This shows that both in the presence and in the absence of 50 wt% DMSO there is a single symmetrical peak centred at 0.424 nm and 0.419 nm, respectively. This pattern is typical of a gel phase in which the hydrocarbon chains are in a fully extended conformation and packed into a hexagonal array. The absence of a shoulder or peak on the high-angle side indicates that the chains are oriented perpendicular to the bilayer surface. It may be concluded from

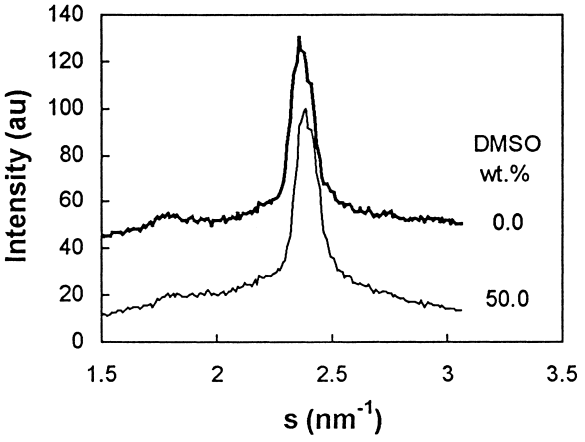

Fig. 8. Wide-angle X-ray diffraction patterns of the POPE dispersions in water and 50 wt% aqueous DMSO solutions. Data correspond to the small-angle diffraction data used to calculate the electron density profiles shown in Fig. 7.

this that the apparent increase in thickness of the bilayer due to the presence of DMSO cannot be due to any change in orientation of the hydrocarbon chains. Thus from the acyl chain spacings it can be seen that the cross-sectional area occupied by each lipid in the bilayer is 0.35 nm^2 and 0.36 nm^2 for dispersions in water and 50 wt% DMSO, respectively.

The effect of DMSO on thermotropic phase behaviour of POPE is consistent with previous studies of phosphatidylcholines dispersed in aqueous DMSO solutions, namely that the temperature of the lamellar-gel to lamellar-liquid-crystalline phase transition increases with increasing DMSO concentration in water. In addition, the present results show that DMSO causes a decrease in temperature of the lamellar to hexagonal-II phase transition which is associated with a significant loss in cooperativity of the transition process.

4. Discussion

The lamellar repeat spacing of the L_β phase of POPE/water dispersion (6.31 nm) is longer than that of dipalmitoylphosphatidylethanolamine (6.03 nm) [24] and shorter than that of distearoylphosphatidylethanolamine (6.35 nm) [25]. The presence of an unsaturated fatty acyl chain does not appear to influence the bilayer repeat dimensions of the lipid in the gel phase. Based on the electron density profiles of lipid multilayers, the distance between the phosphorus atoms located on either side of the bilayer can be estimated from the peak-to-peak distance and a value of 5.02 nm for the POPE/water dispersion in L_β phase was obtained (Fig. 7). This value, however, is not the actual thickness of the bilayer because the dimension of the substituent attached to the phosphate is not taken into account. It is recognised that the precise boundary between lipid and solvent is not discrete but consists of a region comprised of the solvated lipid head groups. Attempts to define the extent of this region based on the molecular weight and specific density of the phospholipid have been made [23,26]. It was concluded that an offset of 0.4 nm should be made between the outer edge of the lipid head groups and the maximum of the electron density profile for phosphatidylethanolamine bilayers in the gel phase state, contributing, in total, 0.8 nm to bilayer thickness. Using this value, the thickness of the solvent layer for fully hydrated POPE was calculated to be 0.49 nm. This agrees well with a value of 0.50 nm reported for fully hydrated dispersions of dilauroylphosphatidylethanolamine in both gel and liquid-crystal phases [23].

In the presence of 50 wt% DMSO, the peak-to-peak distance from the electron density profile of POPE in the L_β phase (Fig. 7) is increased by 0.68 nm to a value of 5.70 nm. This is similar to our previous measurements of DPPC in which DMSO was shown to have caused an apparent increase in thickness of the bilayer in the gel state [15]. In the absence of evidence from WAXS of any change in the angle of tilt of the hydrocarbon chains induced by DMSO it could be inferred that a preferred location and/or arrangement of DMSO molecules about the lipid polar head groups may contribute to the X-ray scattering from this region of the structure. The electron density calculation shows that the solvent layer in the POPE/DMSO aqueous dispersion was abolished when the concentration of DMSO is 50 wt%.

The apparent thickening of the lipid bilayer and disappearance of the solvent layer in the presence of 50 wt% DMSO can be explained if the relatively heavy sulphur atoms of DMSO contribute to the X-ray scattering. Randomly oriented DMSO and water molecules scatter X-rays with approximately the same intensity in the small-angle region according to the atomic scattering factors of the individual atoms and the specific density of the two solvents [27]. When considered individually, the sulphur atoms of DMSO would contribute more significantly than other atoms such as oxygen, carbon, and hydrogen. This is because the atomic scattering factor of sulphur is twice that of oxygen at zero scattering angle, and this ratio only reduces to 1.92 ($=13.6/7.1$) when the angle increases to $\sin\theta/\lambda = 1$ nm^{-1}, an angle reflecting the fifth or sixth order of the SAXS. In order for the sulphur atoms of DMSO to contribute to the X-ray scattering from the lipid–solvent interface the sulphur atoms would need to be located about the polar head groups of the lipid molecules. This may require strong hydrogen bonding to the phosphate group possibly by replacement of water molecules hydrating this group. Gor-

deliy et al. [9] have pointed out that the extent of the shift of electron density maximum towards the solvent domain cannot be larger than the length of the S=O bond (approximately 0.15 nm) giving a maximum increase in bilayer thickness of about 0.3 nm. The value we obtained for the increase in bilayer thickness for DPPC bilayers dispersed in 35 wt% DMSO was 0.22 nm [14], well within the theoretical limits prescribed by the dimensions of the DMSO molecule.

Two differences between phosphatidylcholines (PC) and phosphatidylethanolamines (PE) dispersed in excess water can be recognised from their electron density profiles. Firstly, the aqueous channel separating successive bilayers within multilayer structures of PE is much thinner than PC [26,28]. Dehydration effects on the lipid assemblies due to the presence of DMSO [5,15] might, therefore, be expected to be very conspicuous in POPE multilayers. Secondly, hydrogen bonds between the sulphonyl oxygen and the phosphate group may occur in both PC and PE dispersed in DMSO solutions but the amino group of PE represents an additional hydrogen bonding site for DMSO. When the sulphur and phosphorus atoms are located in the interfacial region they could both contribute to the electron density profile shown in Fig. 7. Thus the calculated dimension of the aqueous layer in L_β phase of POPE is only 0.49 nm and, by analogy with DPPC, the solvent layer could be reduced to such an extent that the opposing lipid head groups meet, leaving solvent molecules only in the interfacial region. This is consistent with the electron density profile of the phospholipid dispersed in excess 50 wt% DMSO when the intervening solvent layer apparently disappears. The true thickness of the bilayer would not be expected to change significantly in the presence or absence of DMSO as, according to the WAXS intensity profile (Fig. 8), the molecules are in a vertical orientation and packed into a regular gel-phase lattice. The precise arrangement of DMSO molecules about the PE head group is presently unknown but possibilities include extension of the two methyl groups into the hydrophobic core of the bilayer with the sulphur atoms oriented towards the interbilayer space or an alignment of the methyl groups with the methylene groups of the ethanolamine.

An increase in the apparent bilayer thickness of DPPC due to the presence of DMSO is in contrast with studies reported by other workers [7,9]. Both these studies found no significant change in the peak-to-peak distance in the lamellar-gel phase of DPPC dispersed in different DMSO concentrations. There was, however, an increase in the apparent bilayer thickness of a subgel phase which was found to form in the presence of DMSO in water in excess of $\chi = 0.07$. Our data for the gel phase was collected immediately after cooling the dispersion from 55 to 25°C which, according to the partial phase diagram published by Tristram-Nagle et al. is very close to the phase boundary between the gel and subgel phase. The WAXS profile in our case shows an unequivocal gel phase with no sharp peak at a spacing of 0.446–0.460 nm typical of the DMSO-induced subgel phase reported by Tristram-Nagle et al. [7]. The temperature conditions used by Gordeliy et al. [9] were not stated but again the WAXS data are consistent with a gel phase which they used for their electron density calculations. One explanation for the discrepancy could be the time scale over which the data was collected. Diffraction patterns can be recorded from synchrotron X-radiation in a matter of seconds whereas, with conventional X-ray generators, accumulation times of hours or days are required to collect equivalent scattering intensities. The longer time for data acquisition may result in relaxation to an equilibrium structure that differs from the phase formed on initial cooling of the dispersion.

Another apparent difference between published electron density profiles of the DPPC/aqueous DMSO system is the relative electron densities of the solvent domain and the region of high electron density associated with the phosphate groups at the lipid–water interface. The peaks of electron density were enhanced by increasing amounts of DMSO when the profiles were referenced to the electron density of the bilayer core [9,15]. This is consistent with orientation of DMSO molecules at the lipid–solvent interface where the sulphur atoms may contribute to the X-ray scattering. By contrast, electron densities at the lipid–solvent interface were found to decrease when water is progressively replaced by DMSO molecules in the calculations reported by Tristram-Nagle et al. [7]. This result is difficult to explain. Even if the electron densities of water, DMSO and their mix-

tures are taken to be the same the electron density of the lipid phosphate region would not be expected to change.

The wide application of DMSO in biology and the pronounced effect it has on the phase behaviour of lipids have also attracted the attention of theorists. Smondyrev and Berkowitz [10], for example, simulated the bilayer properties of DPPC using a molecular dynamics approach. Their results supported earlier conclusions that DMSO reduces the repulsion force between opposing bilayers [14]. The simulation, however, failed to generate any change of bilayer thickness that was expected when DMSO molecules replaced water hydrating the polar head group of the lipid. This could be due to a number of problems inherent in the molecular dynamics method. Firstly, the time scale used in the study, 2 ns, might not be sufficient to mimic the steady-state situation. As pointed out in a recent review [16], a few nanoseconds is too short for the molecular dynamics method to simulate slow processes such as permeation of solvent molecules into bilayers and co-operative motions in phase transitions. It could be argued, therefore, that the simulation time of 2 ns used by Smondyrev and Berkowitz [10] is not long enough to produce a bilayer that differs significantly from the initial configuration as is the case for most molecular dynamics simulations undertaken so far [16]. Secondly, the temperature nominated for the simulation (50°C) so as to ensure the dispersions of DPPC in both water and DMSO are in the liquid-crystal state is not correct. It is true that in water the main transition temperature of DPPC is around 41.5°C but when dispersed in pure DMSO, DPPC has a main phase transition at about 52°C [14]. Thus their simulation on DPPC/DMSO system was actually performed in a lamellar-gel phase.

The present results of the effect of DMSO on POPE are consistent with our earlier studies of the structure of DPPC bilayers in the presence of DMSO. One particular feature is the apparent shrinkage of the intervening solvent layer in multilayer structures of both phospholipids. The effect of DMSO on phase behaviour is also similar for the two phospholipid classes. This suggests that the effect of DMSO on membrane function are not dependent on specific interactions with membrane phospholipids but rather as a general effect on hydration of the membrane surface.

Acknowledgements

Dr Xiaoyuan Wang is thanked for assistance in construction of the swelling series and for helpful discussions. Partial financial support from the National Science Foundation of China (NSFC) and discussions with Dr Tieleman on molecular dynamics are acknowledged by Z.W.Y.

References

[1] N.M. Tsvetkova, P.J. Quinn, in: A.R. Cossins (Ed.), Temperature Adaptation of Biological Membranes, Portland Press, London, 1994, pp. 49–62.
[2] L.M. Crowe, D.S. Reid, J.H. Crowe, Biophys. J. 71 (1996) 2087–2093.
[3] R. Koynova, J. Brankov, B. Tenchov, Eur. Biophys. J. Biophys. Lett. 25 (1997) 261–274.
[4] N.M. Tsvetkova, B.L. Phillips, L.M. Crowe, J.H. Crowe, S.H. Risbud, Biophys. J. 75 (1998) 2947–2955.
[5] M.A. Kiselev, P. Lesieur, A.M. Kisselev, C. Grabielle-Madelmond, M. Ollivon, J. Alloys Compounds 286 (1999) 195–202.
[6] T.J. Anchordoguy, J.F. Carpenter, J.H. Crowe, L.M. Crowe, Biochim. Biophys. Acta 1104 (1992) 117–122.
[7] S. Tristram-Nagle, T. Moore, H. Petrache, J.F. Nagle, Biochim. Biophys. Acta 1369 (1998) 19–33.
[8] Z.W. Yu, P.J. Quinn, Mol. Membr. Biol. 15 (1998) 59–68.
[9] V.I. Gordeliy, M.A. Kiselev, P. Lesieur, A.V. Pole, J. Teixeira, Biophys. J. 75 (1998) 2343–2351.
[10] A.M. Smondyrev, M.L. Berkowitz, Biophys. J. 76 (1999) 2472–2478.
[11] D.S. Hsieh (Ed.), Drug Permeation Enhancement, Theory and Applications, Marcel Dekker, Dortmund, 1994.
[12] Z.W. Yu, P.J. Quinn, Biosci. Rep. 14 (1994) 259–281.
[13] F. Casali, V. Burgat, P. Guerre, Rev. Med. Vet. 150 (1999) 207–220.
[14] Z.W. Yu, P.J. Quinn, Biophys. Chem. 70 (1998) 35–39.
[15] Z.W. Yu, P.J. Quinn, Biophys. J. 69 (1995) 1456–1463.
[16] D.P. Tieleman, S.J. Marrink, J.C. Berendsen, Biochim. Biophys. Acta 1331 (1997) 235–270.
[17] L.J. Lis, P.J. Quinn, J. Appl. Crystallogr. 24 (1991) 48–60.
[18] D. Sayre, Acta Crystallogr. 5 (1952) 843.
[19] P. Laggner, Top. Curr. Chem. 145 (1988) 173–202.
[20] P.W. Sanderson, L.J. Lis, P.J. Quinn, W.P. Williams, Biochim. Biophys. Acta 1067 (1991) 43–50.
[21] M. Jaworsky, R. Mendelsohn, Biochemistry 24 (1985) 3422–3428.

[22] B. Perly, I.C.P. Smith, H.C. Jarrell, Biochemistry 24 (1985) 1055–1063.
[23] T.J. McIntosh, S.A. Simon, Biochemistry 25 (1986) 4948–4952.
[24] B.G. Tenchov, L.J. Lis, P.J. Quinn, Biochim. Biophys. Acta 942 (1988) 305–314.
[25] W.P. Williams, P.J. Quinn, L.I. Tsonev, R.D. Koynova, Biochim. Biophys. Acta 1062 (1991) 123–132.
[26] T.J. McIntosh, S.A. Simon, Annu. Rev. Biophys. Biomol. Struct. 23 (1994) 27–51.
[27] B.D. Cullity, Elements of X-ray Diffraction, 2nd edn., Addison-Wesley, London, 1978.
[28] S. Leikin, V.A. Parsegian, D.C. Rau, R.P. Rand, Annu. Rev. Phys. Chem. 44 (1993) 369–395.